

Compatibility of Inconel 617® Alloy with LiF-MgF_2-KF Thermal Energy Storage Salts and Vacuum at High Temperature

A. Luo, D.L. Jacobson, and R. Ponnappan

Thermal energy storage capsules made of Inconel 617* alloy were filled with high-purity LiF-MgF_2-KF salts and thermally cycled at 983 ± 100 K in vacuum for up to 5 years. The containment life performance characteristics with fluoride salts and in vacuum were examined. Metallographic study indicated that the inside surfaces of the post-test containers had a corrosion damage of 100 μm in depth after 5 years of thermal cycling. The outer surface showed a vaporization damage of 120 μm after the same period. After 5 years of thermal cycling, the aluminum concentration at the capsule interior surface was reduced to 0.424 wt% from a nominal concentration of 1.34 wt% and chromium was reduced to 18.7 wt% from a nominal concentration of 21.8 wt%. A more significant depletion of aluminum and chromium was observed at the outer surfaces. Atomic absorption spectroscopy (AAS) and differential thermal analysis (DTA) were used to reveal the alloying element dissolution and the changes in melting temperature and heat of fusion of fluoride salts during thermal cycling. A modified diffusion equation for a one-dimensional semi-infinite bar was applied to the depletion of aluminum on the interior surfaces of the containers. Good agreement was obtained between the analysis and the measured concentration profiles.

1. Introduction

THE idea of thermal energy storage (TES) in the form of latent heat of fusion has attracted scientists working on solar energy space power systems. This form of energy storage is advantageous with respect to other energy storage forms because of the high specific heat per unit volume, small temperature variation, and high efficiency. Solid-to-liquid phase change is an ideal form of thermal energy storage because the energy density (kJ/g) is much greater than the solid-to-solid phase changes and also because high strength containment is not necessary for the pressure buildup that occurs during the transformation from liquid to vapor. Multicomponent eutectic fluoride salts with melting points in the neighborhood of 1000 K and heats of fusion well above the minimum requirement of 0.4 kJ/g[1] are strong candidates for thermal energy storage application.

The selection of thermal capsule container materials was based on compatibility of the alloy with fluoride salts and with vacuum at elevated temperatures. In space, the evaporation of alloying elements with high vapor pressures leads to a change in composition and potential reduction in the corrosion resistance and lifetime of the capsules. In the fluoride salt environment, alloying elements may diffuse into, and react with, the salt thereby weakening the container wall, thus promoting failure in long-term operation. Thermodynamic calculations by Misra[1] formed the basis for the selection of Inconel 617 (Ni-21.8Cr-12.6Co-8.6Mo-1.34Al-0.2Ti by weight percent) as the containment material for the thermal energy storage capsules in the present research. Compatibility of Inconel 617 with fluoride salts was examined in an earlier program.[2] No significant corrosive attack was observed after 2000 h of testing. However, the compatibility of Inconel 617 with fluoride salts and with vacuum at high temperatures, especially under long-term thermal cycling, needed to be established, and the present experiment was designed to provide the extended lifetime performance characteristics of Inconel 617 alloy with fluoride salts and with vacuum.[2,3]

2. Experimental Procedure

The experimental procedure consisted of processing ultrapure eutectic fluoride salts and thermal energy storage containers under controlled conditions. Ultrapure fluoride salts LiF, MgF_2, and KF were supplied by Ventron Corp. in tightly packed plastic bottles filled with an argon/nitrogen atmosphere. The composition of the eutectic salts was 63.5LiF-30.5MgF_2-6KF (molar percent), or 42.2LiF-48.8MgF_2-9KF (weight percent). The salts were then weighed and mixed inside a glove box that was maintained with contamination levels of oxygen and moisture below 3 and 0.2 ppm, respectively. Salts were melted *in situ* under an argon gas atmosphere in a 1-in. diameter and 3 in. long metal capsule fabricated from extruded Inconel 617 tube and bar stock. Figure 1 is a schematic of the capsule dimension and the inside salts. To allow for liquid expansion, 45 g of salts was placed in each capsule. The capsules were sealed by electron beam welding of the end caps in vacuum[4].

The thermal energy storage capsules thus formed were placed horizontally in a tubular Lindberg temperature-controlled electric furnace for continuous thermal cycle/life testing by cycling over 983 K (eutectic temperature of the salt mixtures) ±100 K every 4 h. A sheathed chromel-alumel thermocouple was attached to each capsule to monitor test temperature. A mechanical pump maintained a vacuum of 20 mtorr in the chamber

*Inconel 617 is a registered trademark of the Inco Alloys International, Inc.

A. Luo and **D.L. Jacobson,** Department of Chemical, Bio, and Materials Engineering, Arizona State University, Tempe, Arizona; and **R. Ponnappan,** Universal Energy Systems, Inc., Dayton, Ohio.

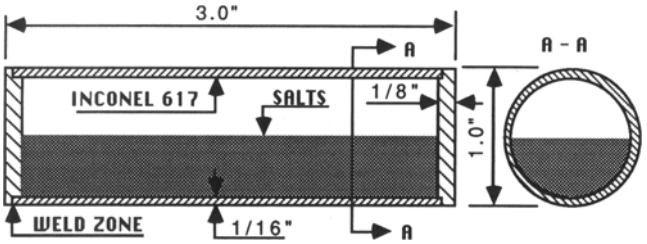

Fig. 1 Schematic of capsule dimensions and inside salts.

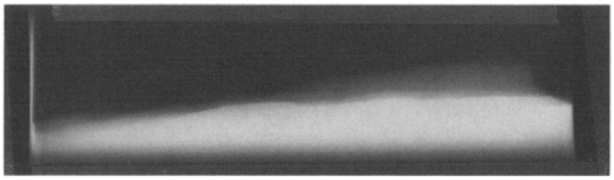

(a)

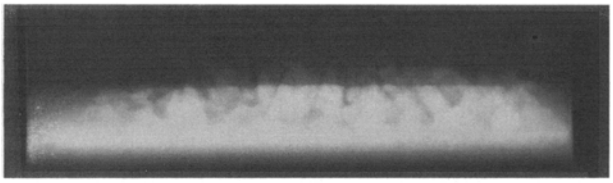

(b)

Fig. 2 X-ray radiographs of 40,000-h (**a**) and 50,000-h capsules (**b**).

at all times. The performance of this test in a vacuum furnace eliminated external corrosion of the capsules and provided for the safety of personnel in the event of a leak or capsule breach. The power input to the furnace was controlled through a set point programmer/timer to switch the system on or off as desired by the thermal cycle requirements. The details of the experimental setup have been published previously.[4]

One of five capsules was removed from the test apparatus after 10,000 h (approximately 1 year) for post-test evaluation. The remaining four capsules were removed at 10,000-h intervals. Extensive metallurgical and chemical analyses were then performed on all post-test capsule containers and eutectic fluoride salts.

3. Analysis

3.1 *X-Ray Radiography*

X-ray radiography is a nondestructive test for revealing macroscopic defects, flaws, and inhomogeneities in materials. X-ray radiography was carried out on the thermal energy storage capsules prior to sectioning. Radiographs were taken with 350-kV X-ray to reveal internal flaws and weld defects in the capsule containers. Figure 2 shows the radiographs taken from thermal energy storage capsules after 40,000 and 50,000 h of lifetime thermal cycling. The regions of higher material density are brighter than the lower material density regions. The solidification profile of the salts is evident in the radiograph. No flaws were observed in any of the thermal energy storage capsule containers within the capability of the instrument resolution.

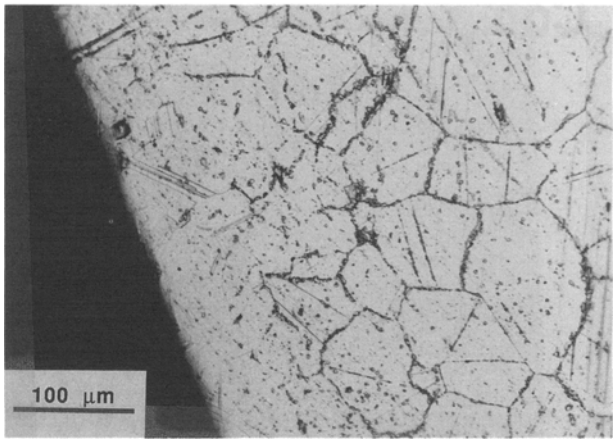

Fig. 3 Microstructure at the inner edge of the 40,000-h specimen.

3.2 *Metallographic Examination*

The capsules were cut into longitudinal and transverse sections for metallographic examination and were selected on the basis of potential criticality. The initial cutting was done by hacksaw to avoid contaminating the salt by coolants and cutting oils. Salt samples from the interior or from regions away from the cut were used for chemical analysis. Visual examination of the salts did not reveal any significant discoloration.

The metallic samples used in microscopy were subsequently cut with a diamond saw to avoid mechanical damage. The metallographic specimens were prepared by further sectioning and cold mounting with Buehler Epo-Kwich resin. The mounted metallography specimens were polished with 320, 400, and 600 silicon carbide grit emery papers followed by fine polishing with 1.0- and 0.05-μm alumina. Samples were then thoroughly cleaned with distilled water and ethanol and etched for optical microscopy examination. Etching was achieved with aqua regia (75 vol% HCl-25 vol% HNO_3).

Microstructural changes in the inner edge (exposed to the molten salts) of all post-test thermal energy storage capsules were studied. Figure 3 shows the metallograph of a thermal energy storage capsule after 40,000 h of thermal cycling. The general microstructure of the post-test specimens consisted of well-defined and large grains of unequal size with the grain boundaries decorated with irregular carbide precipitates. Some were blocky, whereas others were elongated in the direction of the grain boundaries. The carbides were identified as either

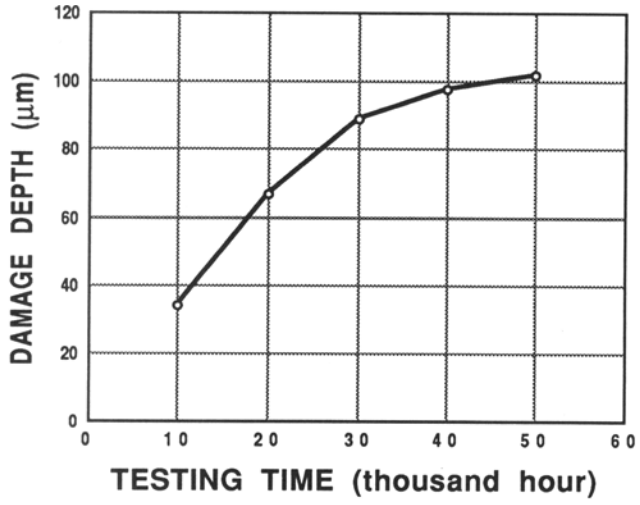

Fig. 4 Damage depth at the inner edge as a function of cycling time.

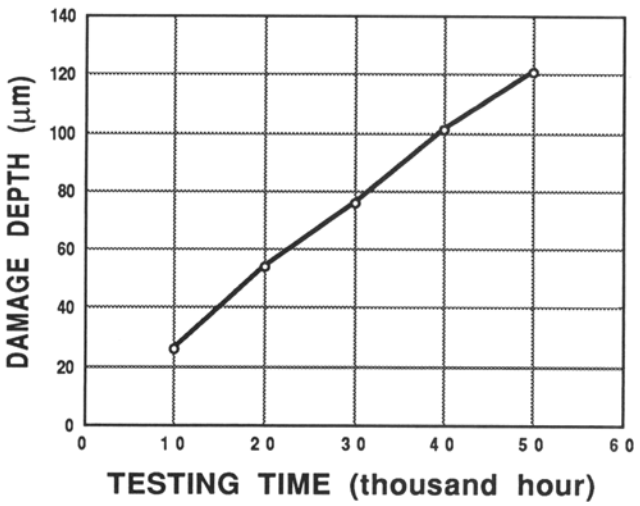

Fig. 6 Damage depth at the outer edge as a function of cycling time.

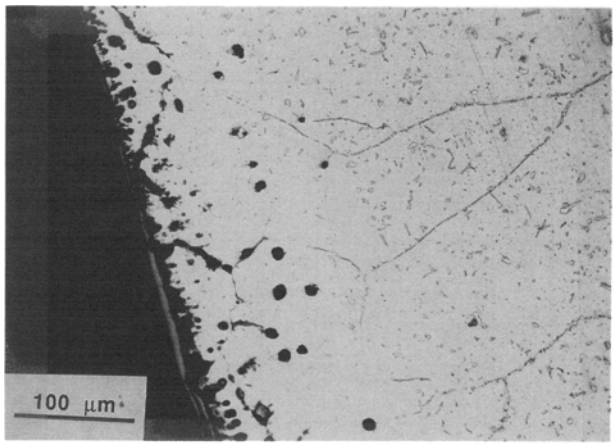

Fig. 5 Microstructure at the outer edge of the 50,000-h specimen.

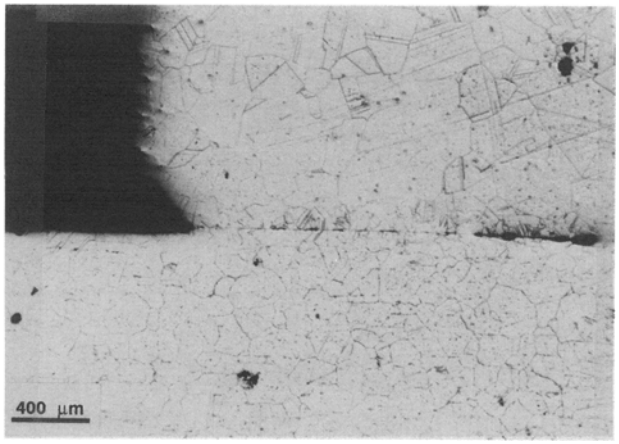

Fig. 7 Welding zone of 30,000-h specimen. Top is the end cap and bottom is the tube.

chromium or molybdenum carbides. The bulk grains also contained some cubical inclusions, which were identified as titanium nitrides.

It was found that the depth of corrosion region was a function of testing time (Fig. 4). Corrosion progressed rapidly during the initial 30,000-h period and then decreased with continued testing, indicating that a protective film was probably formed. After 50,000 h of thermal cycling, the damage depth at the inner surface of the specimen was approximately 100 μm.

The outer edge of the specimen, which was exposed to a 20-mtorr vacuum, also showed microstructural damage. Figure 5 is a metallograph of the outer edge of the 50,000-h specimen. The damage at the outer edge of thermal energy storage capsules was believed to be associated with the material vaporization at high temperatures when exposed to vacuum during long-term operation. Figure 6 shows the progressive damage depth during thermal cycling. Because no protective film was formed at the outer surface, the damage depth progressed approximately linearly with cycling time. The damage depth at the outer surface was determined to be 120 μm after 50,000 h of thermal cycling. Precipitates observed along grain boundaries were identified as sigma phase.

The thermal energy storage capsules were fabricated by electron beam welding an Inconel 617 tube at both ends with caps. In approximately half of the thermal energy storage capsules fabricated, there was a gap between the end cap and the tube wall. Figure 7 is a typical example. The existence of this gap was possibly due to the design, the machined fit, or insufficient weld penetration. Such a region between the end cap and tube should be eliminated so that the expansion of salts during melting does not result in gap growth, leading to catastrophic failure during service. The gaps in the tube/cap weld region would probably be the weakest points of the capsule structure. Increasing welding penetration and changing the cap/tube interface design is strongly suggested.

3.3 *Energy-Dispersive X-Ray Spectroscopy*

The precipitates and inclusions in the microstructure were qualitatively identified by energy-dispersive X-ray spectroscopy (EDS) from the area of interest. From the EDS spectra analysis, most of the precipitates lining the grain boundaries were identified as being either chromium or molybdenum carbides. These precipitates are known from the literature[5] to be either M_6C or $M_{23}C_6$ carbides, where M refers to chromium or molybdenum.

It is known from the literature[6] that the untested Inconel 617 alloy does not produce grain boundary precipitates. It was therefore concluded that the grain boundary precipitates were formed during high-temperature testing. The cubical precipitates, which appeared to be darker than others, were identified as titanium rich, most probably titanium nitride.

3.4 *Differential Thermal Analysis*

The melting temperature and heat of fusion of all post-test eutectic salts were determined by differential thermal analysis (DTA). The results are given in Table 1. There was no significant change in the melting temperature during thermal cycling. The melting temperature of the eutectic salts dropped 5° after 5 years of thermal cycling. The slight decrease in melting temperature was attributed to the dissolution of container materials into the salts by a high-temperature diffusion-controlled corrosion processes. As shown in Table 1, the heat of fusion for the post-test salts was also found to be lower than for the initial salts. The heat of fusion decreased with increasing thermal cycling time. Such a change in heat of fusion was also thought to be associated with the dissolution of impurities into the eutectic salt mixture.

Table 1 Physical properties of post-test salts as a function of testing time

Testing time, h	Melting point, K	Density, g/cm^3	Heat of fusion, J/g
0	983.0	2.970	...
10,000	981.5	2.976	492.4
20,000	980.5	2.985	485.9
30,000	979.0	2.998	480.2
40,000	978.5	3.003	476.0
50,000	978.0	3.005	474.3

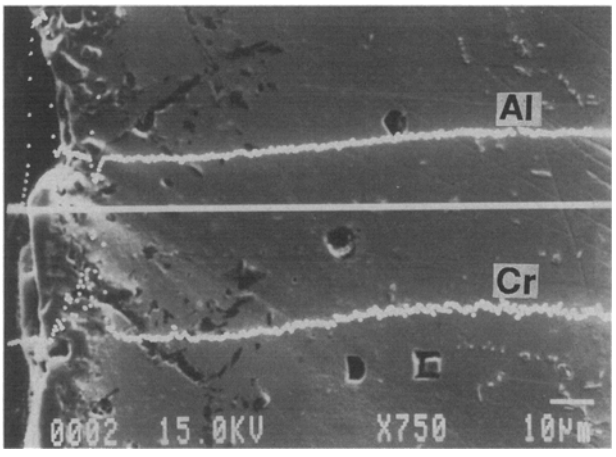

Fig. 8 X-ray linescan of aluminum and chromium at the inner edge of post-test thermal energy storage capsule.

3.5 *Electron Probe Microanalysis*

The results obtained by differential thermal analysis strongly suggested that some alloying elements were dissolved into the salts during long-term thermal cycling at high temperatures. Figure 8 is an X-ray linescan of aluminum and chromium across the inner edge of a post-test thermal energy storage capsule. There was a drop in the signals near the edge, indicating the depletion of these two elements. Quantitative measurements were therefore performed at various points on the con-

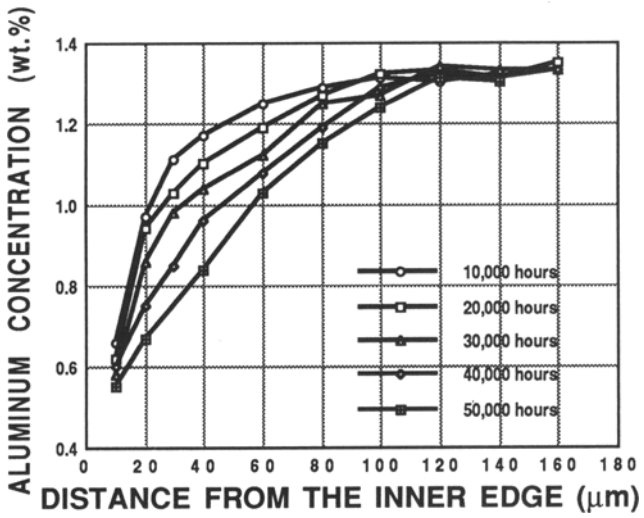

Fig. 9 Aluminum profile near the inner edge.

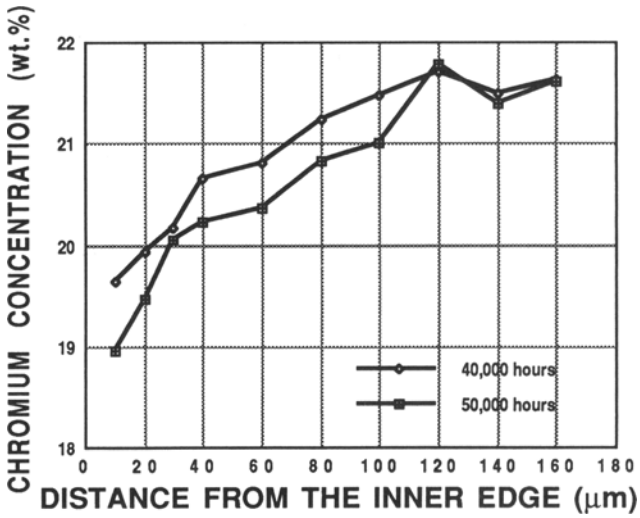

Fig. 10 Chromium profile near the inner edge.

tainer wall with an electron probe microanalyzer (EPMA), which consisted of an electron source and detection systems for X-rays.

Standards were used in determining the composition profile across the wall thickness. Compositions, in weight percent, were obtained at intervals of 10 to 20 μm across the container edge with a beam diameter of 2 μm. Spots very near precipitates or voids were avoided to prevent signals of those features from interfering with the bulk analysis. An optical microscope was attached, the focusing of which ensured that the area of interest was sufficiently flat for reliable spectrometer readings.

The composition profiles of aluminum, chromium, and molybdenum across the wall were determined for all tested thermal energy storage capsules. Figures 9 and 10 show the aluminum and chromium profiles near the inner edges of tested thermal energy storage capsules. The depletion of both elements developed with increased testing time. However, the concentration at depths greater than 120 μm from the edges was approximately a time-independent constant, close to the nominal compositions. A similar depletion phenomenon of aluminum and chromium was also observed near the outer edges of tested thermal energy storage capsules due to the high-temperature evaporation in vacuum, as shown in Fig. 11 and 12.

The composition at both inner and outer surfaces was obtained by curve fit of the data determined by EPMA. It was found that there was a significant reduction in the quantities of aluminum and chromium at the inner and outer surfaces of post-test capsules. For the 50,000-h thermal energy storage capsule, aluminum concentration was reduced from a nominal concentration of 1.34 to 0.42 wt% at the inner surface and to 0.13 wt% at the outer surface. At the same time, chromium concentration was reduced from a nominal concentration of 21.8 to 18.7 wt% at the inner surface and to 13.2 wt% at the outer surface.

As shown in Fig. 13, molybdenum behaved opposite to aluminum and chromium. The concentration of molybdenum near the edges was higher than the nominal composition. When moving inward from the edge, the molybdenum concentration decreased and finally reached the nominal composition. This behavior suggested that molybdenum diffused from the interior area to the surface at high temperatures. The driving force for the molybdenum diffusion was believed to be the vacancy differential between the center area and the subsurface where the depletion of aluminum and chromium left numerous vacancies.

3.6 *Chemical Analysis*

The salt was analyzed to detect the presence of alloying constituent that may have been leached out or dissolved. Determination of the presence of metallic elements in the salt was not possible with EPMA. A difficulty encountered in obtaining accurate results from the microprobe was that elements in the salt may have been present only in a particular phase of the eutectic structure. Hence, additional chemical analyses were conducted

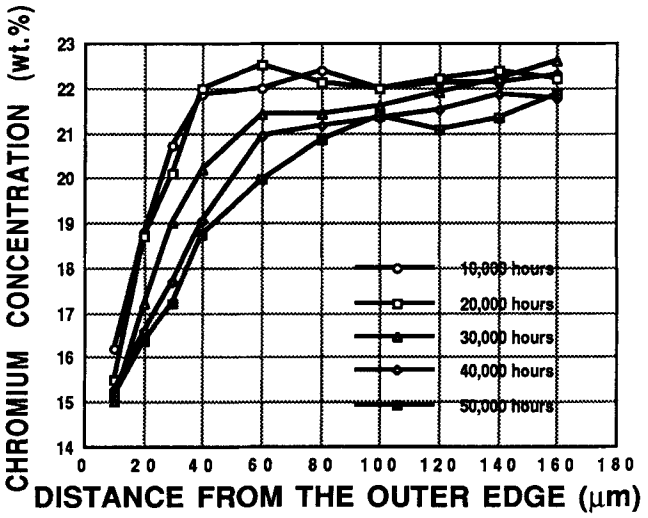

Fig. 12 Chromium profile near the outer edge.

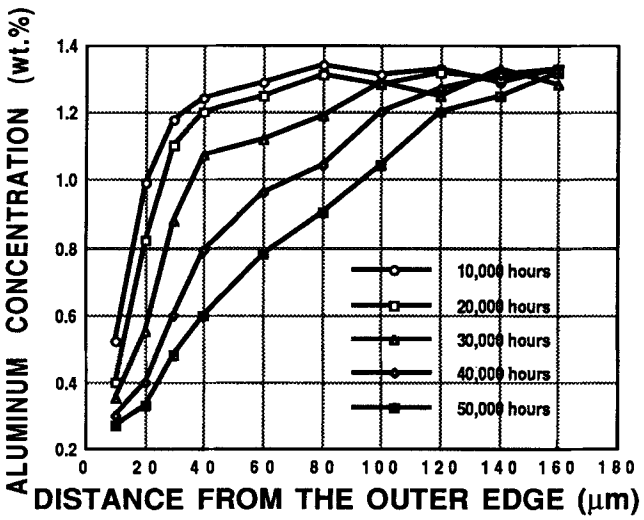

Fig. 11 Aluminum profile near the outer edge.

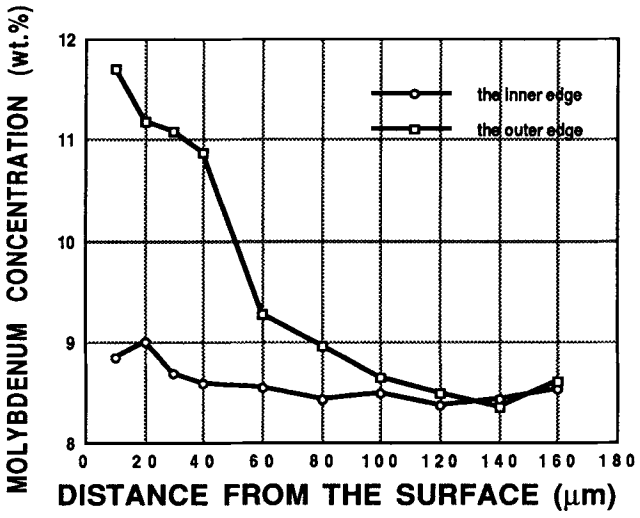

Fig. 13 Molybdenum profile near the inner and outer edge after 50,000 h of thermal cycling.

Table 2 Weight percentage of aluminum and chromium in salts during thermal cycling

Testing time, h	Aluminum, wt%	Chromium, wt%
0	0.00	0.000
10,000	0.31	0.034
20,000	0.24	0.113
30,000	0.28	0.046
40,000	0.23	0.034
50,000	0.30	0.024

Table 3 Comparison of aluminum concentrations determined by EPMA and calculated from the diffusion equation

Distance from the inner edge, μm	EPMA	Theory	Error, %
0	0.424	0.419	1.19
10	0.551	0.539	2.22
20	0.669	0.660	1.36
40	0.840	0.874	-3.89
60	1.031	1.047	-1.53
80	1.142	1.171	-2.48
100	1.240	1.252	-0.96
120	1.308	1.298	0.77
140	1.310	1.322	0.91

for the detection of aluminum and chromium in the salts by using atomic absorption spectroscopy (AAS).

The quantitative analysis for aluminum and chromium concentration in salts was conducted with a flame AAS using primary standards. The salt samples were dissolved in concentrated nitric acid and digested for 6 h followed by subjecting the solution to flame spectroscopy. The results are presented in Table 2. Both aluminum and chromium were detected in the post-test salts, confirming that these alloying elements were dissolved in the molten salts during long-term thermal cycling at high temperatures.

4. Discussion

The purpose of the present experiment was to determine the effect of eutectic salts on the containment metals. The results of the various detailed analyses indicated that the corrosion effects were not severe, even after 50,000 h of thermal cycling. The removal of aluminum and chromium from the thermal energy storage containers can be considered in light of thermodynamic calculations performed by Misra and Whittenberger.[7] In their model, one mole of pure salt LiF, KF, or MgF_2 reacts with pure metals at both ideal and nonideal conditions. The results indicate that the equilibrium amount of aluminum salts will be the highest, followed by chromium, when considering all elements constituting Inconel 617.

Simple dissolution of the pure metal in the salt is not expected except in their own salts, and hence, it is more probable that these elements leached out by direct reaction with the salts. The individual reactions predicted are:

$$6\,MF(l) + Al \rightarrow M_3AlF_6\,(1) \qquad [1]$$

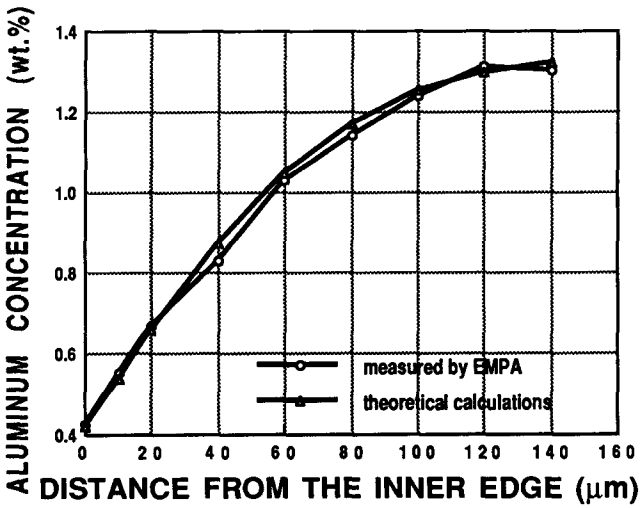

Fig. 14 Comparison between the measured and calculated aluminum profiles for 50,000-h thermal energy storage capsule.

$$2\,MF\,(1) + Cr \rightarrow CrF_2 + 2M\,(1) \qquad [2]$$

where M is Li or K. If M is Mg, the reactions are:

$$3\,MgF_2\,(1) + 2\,Al \rightarrow 2\,AlF_3\,(1) + 3\,Mg\,(1) \qquad [3]$$

$$MgF_2\,(1) + Cr \rightarrow CrF_2 + Mg\,(1) \qquad [4]$$

The concentration profile of aluminum across the tube wall near the inner edge, as shown in Fig. 8, was observed to very closely resemble the solid-state diffusion curve of a binary system.[8] The test data for the 10,000-h capsule were previously modeled as a diffusion curve of a binary system in a one-dimensional semi-infinite bar.[9] This model resulted in a D value of $1.0 \times 10^{-13}\,cm^2/s$, where D is the diffusion coefficient of aluminum in Inconel 617.

Using this D value in the diffusion equation for a testing time of 50,000 h, the following equation was obtained:

$$C_X = C_S + (C_O - C_S)\,\mathrm{erf}(0.5\,(Dt)^{-1/2}X) \qquad [5]$$

where X is the distance (cm) from the inner surface, C_S is aluminum concentration at the inner surface, C_X is aluminum concentration at a distance X from the inner surface, C_O is the nominal concentration of aluminum in Inconel 617, and t is the testing time in seconds.

The aluminum concentration at the inner edge of the 50,000-h capsule was 0.424%, as determined by curve fitting the EPMA results. For the 50,000-h capsule, $t = 1.8 \times 10^8$s. Therefore, the above equation becomes:

$$C_X = 0.424 + 0.921\,\mathrm{erf}(117.85 \cdot X) \qquad [6]$$

The values of C_X at various positions from the inner edge were calculated from Eq 6. In Table 2 and Fig. 14, the theoretical values are compared with the results determined by EPMA. Good agreement is obtained between the experiments and theory. The calculated values from Eq 6 closely fit the determined concentration profile with an error range of ±4%. Therefore, it

was concluded that the corrosion of Inconel 617 in molten fluoride salts is a diffusion-controlled process.

The concentration profiles indicated that chromium was the only other alloying element of Inconel 617 that showed a reduction near the surface. A very small amount of chromium (approximately 1×10^{-4} wt%) of chromium was identified in the post-test salts by AAS analysis. According to the thermodynamic calculations, the equilibrium concentration of chromium in the present flouride salts was 1.6×10^{-3} wt%. Therefore, the equilibrium concentration of chromium had not been reached. It can thus be stated that the corrosion rate of chromium is minimal. This is not of serious concern because a minor depletion of chromium will not cause a significant degradation in the physical properties of Inconel 617.

The outer edge of the wall that was in constant exposure to a vacuum of 20 mtorr at high temperatures showed some microstructural damage consisting of voids and some elongated and irregular inclusions. The EPMA conducted on those regions showed a strong depletion of both aluminum and chromium from the matrix. The most probable reason was vaporization of elements from the Inconel 617 matrix. Vapor pressure calculations were made to predict the vaporization tendencies. At 1100 K, the vapor pressures of alloying elements in Inconel 617 increased in the following order: molybdenum, cobalt, nickel, chromium, and aluminum. Assuming that the vaporization rates are proportional to their vapor pressures, it was not difficult to realize that aluminum and chromium showed the most serious depletion among the alloying elements in Inconel 617.

Formation of voids at the subsurface of thermal energy storage capsules can be explained principally by the movement of vacancies, that is, neighboring atoms move to occupy vacant sites. When an atom is vaporized on the outer surface, the atom below the surface moves to occupy the vacancy and produces another vacancy under the surface. This process creates a flow of vacancies to the subsurface. Subsurface voids are formed through clustering of vacancies.

5. Conclusion

The thermal energy storage capsules filled with eutectic fluoride salts showed minimal degradation and no sign of failure after 5 years of thermal cycling. The inner edge (exposed to the salts) of post-test thermal energy storage capsules sustained corrosion damage of 100 μm in depth after 5 years of thermal cycling. The outer edge (exposed to vacuum) sustained a vaporization damage of 120 μm during the same period. Electron probe microanalysis showed that on the capsule inner surface aluminum concentration reduced to 0.42 wt% from a nominal concentration of 1.34 wt% and chromium reduced to 18.7 wt% from a nominal concentration of 21.8 wt% after 5 years of thermal cycling. Both aluminum and chromium were identified to be dissolved in the fluoride salts at high temperatures.

The depletion of aluminum and chromium at the outer edge was attributed to the high vaporization rates of these two alloying elements in vacuum at elevated temperatures. A slight decrease in the melting temperature and in the latent heat of fusion for the eutectic salts was observed during the lifetime testing of thermal energy storage capsules. This was attributed to the diffusion of alloying elements of container material into the molten salts. A gap between the tube and the end cap was observed in some thermal energy storage capsules. Increased welding penetration and improved end cap design are strongly suggested.

A modified diffusion equation based on the assumption of constant surface concentration at the end of a one-dimensional semi-infinite bar was applied to the depletion of aluminum near the inner edge of specimens thermal cycled for 5 years. The values calculated from this equation closely matched the concentration profile determined by EPMA with an error range of less than 4%, indicating that the corrosion was a diffusion-controlled process. The projected lifetime of 5 to 7 years is reasonable, and the capsules should easily perform their intended function well beyond the required lifetime.

Acknowledgments

This work was supported by the USAF, WRDC, AFAPL, Dayton, Ohio, through Texas A & M Research Foundation, Texas, under contract No. F33615-86-C-2723. The authors would like to thank Mr. J. Clark for the use of the analytical electron microprobe, which was purchased with the aid of NSF grant EAR 8408163, in the Chemistry Department of Arizona State University. The authors would also like to thank Dr. M. Mckelvy and Mr. T.W. Karcher for the use of the TGA/DTA thermal analysis system in the Center for Solid State Science at Arizona State University.

References

1. A.K. Misra, *J. Electrochem. Soc.*, Vol 25, 1988, p 850-861.
2. J.E. Beam, Technical Report AFAPL-TR-75-92, Part II, Mar 1977.
3. E.J. Davison, Technical Report AFAPL-TR-75-92, Part I, Oct 1975.
4. R. Ponnappan, J.E. Beam, V.J. Griethuysen, and E.T. Mahefkey, Proc. 20th Intersociety Energy Conversion Engineering Conference, Vol 2, 1985, p 416-423.
5. C.T. Sims and W.C. Hagel, *The Superalloys*, John Wiley & Sons, 1972, p 121-123.
6. J.W. Koger, *Adv. Corr. Sci. Technol.*, Vol 5, 1975, p 245-256.
7. A.K. Misra and J.D. Whittenberger, *J. Mater. Engr.*, Vol 9, 1987, p 293-306.
8. R.C. Weast, *Handbook of Tables for Mathematics*, 4th ed., CRC Press, 1975, p 920-921.
9. M. Krishnamurthy, D.L. Jacobson, R. Ponnappan, and J. Johnson, *J. Mater. Eng.*, Vol 11, 1989, p 283-290.